Available online at www.sciencedirect.com

ScienceDirect

Procedia Engineering 2 (2010) 3–26

Procedia Engineering

www.elsevier.com/locate/procedia

Fatigue 2010

Fatigue, an everlasting materials problem - still en vogue

Hael Mughrabi*

Department of Materials Science and Engineering, University of Erlangen-Nürnberg, Martensstr. 5, 91058 Erlangen, Germany

Received 5 March 2010; revised 10 March 2010; accepted 15 March 2010

Abstract

In the first part, some fundamental issues that have been under discussion for a long time will be revisited, namely the effect of the cyclic slip mode on the fatigue-induced dislocation distributions, the origin and effect of cyclic slip irreversibilities and their relation to fatigue life and, finally, cyclic strain localization and fatigue crack initiation in persistent slip bands. In the second part, some topics that have recently found increasing interest will be discussed such as the cyclic deformation and fatigue behaviour of ultrafine-grained and nanostructured materials and the microstructural mechanisms that govern fatigue life of ductile and high-strength materials in the range of ultrahigh cycle fatigue. Some general conclusions will be drawn.

Keywords: Cyclic slip mode; cyclic slip irreversibilities; microstructural effects; ultrafine-grained metals; Ultrahigh Cycle Fatigue (UHCF); fatigue lives

1. Introduction

Fatigue research has been one of the prime materials themes for almost 150 years. It has not lost any of its importance, be it in failure analysis, materials characterization and development or in engineering design. But being a traditional discipline, and competing with some novel and currently more fashionable fields as, for example, nano- or bioscience, it frequently nowadays only attracts public interest in the event of a spectacular materials failure. However, for those who are active in the field, fatigue research has remained as fascinating as ever, be it because of increasing importance of new materials which pose new problems or because, with today's improved experimental facilities and computational means, long-standing issues can be dealt with in a more conclusive manner than hitherto. In this sense, not much has changed since the beginning of the International Fatigue Congress series almost 30 years ago, when colleagues like the late Jim Beevers [1] to whose memory this paper is dedicated made lasting contributions to the advancement of the understanding of simple and complex materials fatigue phenomena.

This paper will revisit some fundamental issues that have been under discussion for a long time and are still awaiting final answers, and it will also address selected other topics that have received increasing attention in recent years. The overall emphasis will be on microstructural effects and fatigue mechanisms. Briefly, the contents will be as follows:

* Corresponding author. Tel.: +49 9131 8527482; fax: +49 9131 8527504
E-mail address: mughrabi@ww.uni-erlangen.de

1877-7058
doi:10.1016/j.proeng.2010.03.003

- Some fundamental problems of cyclic plasticity and fatigue revisited
- Fatigue of ultrafine-grained (and nanocrystalline) metals
- Ultrahigh cycle fatigue of ductile and strong materials
- Concluding remarks

2. Some fundamental problems of cyclic plasticity and fatigue revisited

2.1. Origin and significance of wavy and planar cyclic slip modes

Since the pioneering work of Feltner and Laird [2], it has become customary to distinguish between the cyclic deformation behaviour of so-called wavy and planar slip materials. In this terminology, wavy slip implies that cross slip can occur easily, whereas in the case of planar slip cross slip is difficult. Probably, the most important aspect of this distinction is that wavy slip materials have a so-called history-independent cyclic stress-strain (CSS) behaviour with a unique CSS curve, whereas the CSS behaviour of planar slip materials is history-dependent. Furthermore, the distinction between cyclically deformed wavy and planar slip materials permits to plot in a systematic manner the types of dislocation distributions, observed as a function of fatigue lives, in the popular maps introduced by Feltner and Laird [3] and modified by Lukáš and Klesnil [4]. Figure 1 shows the "dislocation distribution map" in the form proposed by the latter but with modified labeling of the ordinate [5]. Originally, the stacking fault energy (SFE) had been plotted on the ordinate, because for many years easy and difficult cross slip had been related to high and low SFE, respectively. This view became untenable, after unequivocal experimental evidence had shown that some materials with rather high SFE can exhibit planar slip. Thus, planar slip was found to occur in alloys having short range order and/or a high yield stress (strong solid solution hardening), as emphasized in ref. [6] and in later papers

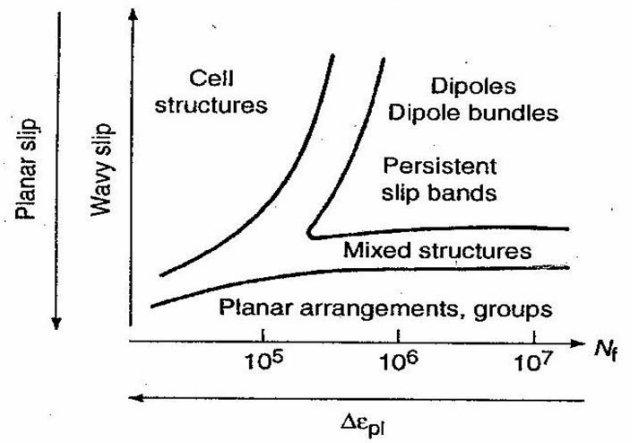

Fig. 1. Dependence of fatigue-induced dislocation patterns on cyclic slip mode and fatigue life. After [5], based on [3,4,9].

[7,8]. In precipitation-hardened alloys, another reason for planar slip can be the cutting of shearable coherent precipitates. In the case of solid solution alloys, the ease or difficulty of cross slip is still regarded as crucial. However, the SFE is no longer considered as the only controlling microstructural parameter. The author, acting as a reviewer, has repeatedly noted that, in particular, the strong overriding effect of short range order in promoting planar slip, almost irrespective of the SFE, has frequently been overlooked even in very recent work. For this reason, the topic has been taken up again. It was Nicole Clement who, more than 25 years ago, first discovered and advocated this effect [9] which was later reviewed and summarized by Gerold and Karnthaler [10]. In consonance with the above, the ordinate in Fig. 1 is now labeled simply in terms of increasing or decreasing ease of cross slip. A good example is recent work on fatigued high interstitial stainless steel, which exhibits short range order and has a

SFE ≈ 37 mJ/m^2 [11], more or less like SFE of wavy slip Cu. Nonetheless, planar slip was observed, unexpected in the traditional version of Fig. 1 (SFE plotted on the ordinate), but understandable in view of the short range order.

2.2. Origin of cyclic slip irreversibilities, relation to fatigue lives

Since the classical work of Ewing and Humfrey [12], it is accepted that the initiation of fatigue cracks at the surface generally arises from the accumulation of unreversed slip steps. This is an indication that to-and-fro dislocation glide is not completely reversible in a microstructural sense and that fatigue damage actually results from the accumulation of a large number of slightly irreversible cyclic microstrains. The glide irreversibility can be characterized by the fraction p of the cumulative irreversible plastic strain with respect to the total cumulative plastic strain [13]. Qualitatively, short and long fatigue lives would be expected to relate to large and small values of the glide irreversibility p, respectively. The development of a quantitative relationship between p and the number of cycles to failure, N_f, would be an ambitious goal. In all probability, a universal relationship of this type does not exist. Rather, it appears probable that different specific relationships exist for different types of failure mechanisms.

In a recent survey, the author has reviewed the different microstructural mechanisms that cause slip irreversibilities, namely annihilation of dislocations, loss of dislocations at the surface, cross slip and, in the case of bcc metals, slip plane asymmetry in tension and compression [13]. Unfortunately, only in a few special cases do sufficiently detailed experimental data exist that permit to deduce under certain assumptions numerical values of the slip irreversibility p. A few examples are listed in Table 1, based on the Table published previously [13] and extended so as to include also fatigue lives N_f where possible. The data are listed for different materials fatigued under constant stress amplitude $\Delta\sigma/2$ or axial plastic strain amplitude $\Delta\varepsilon_{pl}/2$. In the few cases concerning fatigued materials containing so-called persistent slip bands (PSBs, see Section 2.3), the data refer to the local plastic shear strain amplitudes in PSBs, $\gamma_{pl,PSB}$. The different methods by which the values of p were assessed are indicated in the last column on the right. The numbered references are those listed in the original publication [13] to which the reader is referred for details. The fatigue lives N_f given in the Table are those stated in the cited publications, with the following exceptions. In the case of PSBs in fatigued copper and Cu-2at.%Co single crystals, no exact fatigue lives can be stated. For copper fatigued below the PSB threshold in the UHCF regime, the mean plastic shear strain amplitude γ_{pl} is stated. In the case of α-iron, the cyclic slip irreversibilities were derived from the single crystal data, as quoted. However, the fatigue lives stated were extracted from work on fatigued α-iron polycrystals [14] for

Table 1. List of cyclic slip irreversibilities $0 < p < 1$, as determined in specific cases by different means from experimental data [12].

Examples, references	**Testing conditions**	**Irreversibility p**	**Evaluation via**
PSBs, copper X-tals[56.88]	$\gamma_{pl,PSB} \approx 10^{-2}$, RT	≈ 0.3	TEM & dislocation model [25,26]
UHCF, copper [34, 35]	$\gamma_{pl} \approx 1.7\times10^{-5}$, RT, $N_f > 10^{10}$	≈ 0.000034	SEM & dislocation model [34,35]
α-brass X-tals [111, 112]	$\Delta\sigma/2 =$ 82 MPa, RT, $N_f = 10^6$ $\Delta\sigma/2 = 118$ MPa, RT, $N_f = 4\times10^4$	≈ 0.005 ≈ 0.03	TEM & computer simul. [26]
PSBs, Cu-2 at.%Co X-tals[114,115]	$\gamma_{pl,PSB} \approx 2.3\times10^{-2}$, RT	≈ 1	TEM & dislocation model[26]
Waspaloy [116]	$\Delta\varepsilon_{pl}/2 = 10^{-3}$, 650 °C, $N_f = 550$	≈ 0.05	TEM: assessment of irreversible shear displacements[26]
α-iron single crystals [121]	$\Delta\varepsilon_{pl}/2 = 5\times10^{-4}$, RT, $N_f = 6\times10^5$ $\Delta\varepsilon_{pl}/2 = 1.5\times10^{-3}$, RT, $N_f = 1.2\times10^5$ $\Delta\varepsilon_{pl}/2 = 6\times10^{-3}$, RT, $N_f = 9\times10^3$	≈ 0.03 ≈ 0.06 ≈ 0.2	dislocation model of shape changes due to slip plane asymmetry [121]

cyclic deformations at strain amplitudes comparable to those used in the work on the single crystals. From Table 1 follows the expected qualitative conclusion that large and small slip irreversibilities relate to large and small loading amplitudes, viz. short and long fatigue lives, respectively. The derivation of quantitative relationships between fatigue life and slip irreversibility, referring to *individual specific damage mechanisms*, remains a task for the future.

2.3. Persistent slip bands, extrusions (and intrusions) and fatigue damage in fatigued fcc metals – current status

2.3.1. Early observations and dislocation models

Cyclic strain localization in PSBs and the initiation of fatigue cracks in fcc metals have received much attention since the pioneering work of Thompson et al. [15]. In passing, it is in place to admit, as noted by Lukáš and Kunz [16], that the significance of fatigue damage by PSBs is somewhat confined to fatigued simple ductile materials and is of much less relevance with respect to the fatigue resistance of structural materials of practical importance. Nonetheless, the work on PSBs has fascinated many researchers and has led to a general advancement of the understanding of dislocation behaviour in fatigued metals. Especially during the last four decades extensive efforts have been made to clarify the conditions under which PSBs evolve, to determine their dislocation microstructures and to assess the governing dislocation mechanisms, compare [17,18,19], in particular in relation to understanding in detail by which dislocation mechanisms the characteristic surface topography responsible for the initiation of fatigue cracks at emerging PSBs evolves. Early studies of the surface relief were mainly confined to optical and later to scanning electron microscopic (SEM) observations of the surface or of sections under an angle to the surface. In these studies, dramatic changes in the surface relief of PSBs in fatigued metals were first revealed by Forsyth on a fatigued age-hardened aluminium alloy [20] and also by Wood's studies of so-called taper sections performed on different fatigued metals [21]. The studies by Cottrell and Hull [22], using the electron microscope replica technique to image the surface relief of fatigue copper mono- and polycrystals were equally important. In particular, these authors showed that the surface relief developed also at low temperatures (4.2 K). This was strong evidence that the evolution of the surface relief occurred by a purely mechanical mechanism. In these early observations, it was found that so-called extrusions (elevations) developed along the PSBs at the surface, and that there were also intrusions (depressions). Moreover, in some of the observations, the impression was gained that extrusions and intrusions developed side by side, i.e. in the form of extrusion-intrusion "pairs", suggesting that intrusions and extrusions form simultaneously and that the intrusions formed somehow by an "inverse" mechanism of extrusion formation.

Based solely on the early surface observations and before transmission electron microscopy (TEM) became available, several dislocation models were proposed most of which were devised to predict the simultaneous pairwise formation of extrusions and intrusions. These models, discussed in detail in subsequent reviews, e.g. [23] and most recently by the author [13], were based on rather specific assumptions which made it questionable whether the dislocation mechanisms envisaged would operate in reality. A model proposed by Mott is an exception [24]. It was the first model in which the cross slip of screw dislocations played an important role. Mott envisaged a screw dislocation which terminates at the surface and slips and cross slips in a closed path around a trapezoid, thereby generating an extrusion by the slip steps formed at the surface. The essential features of this hypothesis, namely that matter is added to the surface by a purely mechanical dislocation mechanism, while in the interior void-like cavities of equivalent volume are formed can still be viewed as correct today. Thus, Mott's model predicts the formation of extrusions, but provides no mechanism for the formation of intrusions, in conformity with the more recent microstructurally based so-called EGM model [19], to be discussed next.

2.3.2. The EGM and Polák models of extrusions (and intrusions), surface roughening and fatigue crack initiation

Later, TEM studies permitted to characterize in detail the dislocation distributions and to assess the governing dislocation mechanisms of cyclic strain localization in PSBs. Based thereupon, the dislocation mechanisms which operate in PSBs and, at the same time, give rise to the surface reliefs observed at emerging PSBs could be identified and cast into models without the need to make unrealistic assumptions. The formulation of quantitative dislocation models is considerably facilitated by the fact that, in very good approximation, the dislocation patterns can be considered to correspond to a state of cyclic saturation. Hence, it follows that a dynamic equilibrium must exist

between defect production and annihilation. This means in particular that the increase of the dislocation density *must* be balanced precisely by corresponding mutual annihilation processes of *both* screw and edge dislocations, as first recognized by Backofen [25]. In a similar fashion, deformation-induced point defects attain a steady-state concentration. Based on the detailed knowledge of the dislocation glide mechanisms in PSBs in cyclic saturation of fcc single crystals, Essmann et al. [19,26] developed a semi-quantitative model (called EGM model subsequently) of the evolution of the surface relief of PSBs. Modifications of the EGM model by Polák [27,28] will be discussed later. While the EGM and the Polák models are essentially based on detailed knowledge of the dislocation processes in fcc copper single crystals, the underlying assumptions are so general that the predictions, perhaps with slight modifications, will also apply to other materials in which PSBs do not necessarily have the ladder structure.

In the EGM model, combinations of *low-temperature* dislocation glide and annihilation processes, detailed in [13,18,19], lead to rapid growth of so-called *static extrusions* of height *e*. The extruded volume matches precisely the volume of vacancy-type defects that accumulate in cyclic saturation. The *local* vacancy defect concentration C_v^{sat} in the dislocation walls (volume fraction $f_w \approx 0.1$) of the ladder structure is established as the result of a balance between annihilations of very close (vacancy) edge dipoles and formation of edge dipoles. C_v^{sat} ist estimated as 6×10^{-3}. Slipping out of so-called PSB-matrix interface dislocations leads to a one-dimensional elongation of the PSB lamella in the direction of the Burgers vector **b**, creating one static extrusion of height *e* on each side of the crystal:

$$e \approx 0.5\, C_v^{sat} f_w \approx 3\times10^{-4}\, D, \tag{1}$$

where *D* is the specimen diameter measured in the direction of the Burgers vector. Thus, it is predicted that the extrusion heights will be the larger, the thicker the fatigued single crystal is. In the case of a polycrystal, *D* would represent the grain size, and the predicted height of an extrusion in a surface grain would be twice as large as according to eq. (1), because only one extrusion would form. Nonetheless, extrusions in polycrystals should be much smaller than in single crystals because the grain size is generally much smaller than the specimen diameter.

The described purely mechanical material extrusion process can operate in particular at low temperatures, as observed [18,22,29]. If diffusional processes can occur, a slower *continuous extrusion growth* is predicted to occur after the rather rapid growth of static extrusions, since vacancies lost to the PSB by diffusion to the matrix are replaced by the glide and annihilation processes described, whereby additional PSB-matrix interfacial dislocations form and glide out. Furthermore, continued cyclic deformation will lead to a gradual roughening of the surface of the extruded PSB material. According to ref. [26,30], the evolution of surface roughness in the PSB can be described by the mean width $\bar{w}$, defined as the largest peak-to-valley spacing, measured parallel to the Burgers vector, as

$$\bar{w} \approx \sqrt{6bhpN\gamma_{pl,PSB}} \tag{2}$$

where *h* denotes the thickness of the PSB studied and $\gamma_{pl,PSB}$ the *local* plastic shear strain amplitude of the PSB. With appropriate values for a PSB in copper of thickness 1 μm, this leads to

$$\bar{w} \approx 1.5\times10^{-3}\sqrt{N} \quad [\mu m] \tag{3}$$

This surface roughening effect should be similar in polycrystals and in single crystals, whereas the extrusion heights *e* should be much smaller in polycrystals than in single crystals. In summary, the EGM model predicts the following sequence of events for fatigued mono- and polycrystals:

- Rapid formation of static extrusions with heights *e* proportional to *D*, as defined above.
- Gradual surface roughening of the extruded material, and
- Continuous growth of extrusions at temperatures at which diffusional processes occur.

The surface profile predicted by the EGM model at low temperatures at which continuous extrusion growth does not occur, is illustrated schematically in Fig. 13. It should be noted that, aside from the valleys in the surface roughness of older PSBs, the EGM model in its original form describes only the development of extrusions but not of intrusions. Polák [27,28] modified the EGM model in some respects, in particular as follows: 1) Because of the diffusion of vacancies from the PSB into the adjacent matrix, intrusions should form in the matrix adjacent to the PSB-matrix interfaces. 2) Furthermore, continuous extrusion growth was predicted to occur over the whole width of

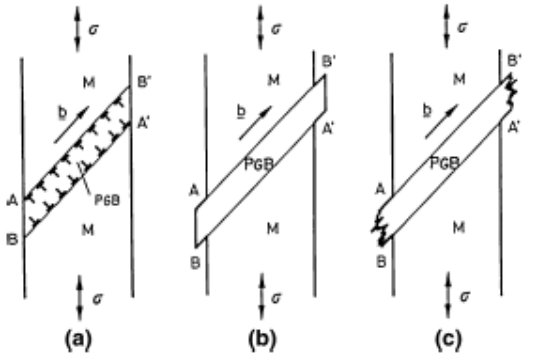

Fig. 2. Schematic illustration of evolution of surface relief at emerging PSB in the absence of diffusional effects. a) Interfacial dislocation accumulate at PSB-matrix interfaces. b) Rapid formation of "static" extrusions by emergence of interfacial PSB-matrix dislocations. c) Gradual roughening of surface of extrusion by random slip in PSB. After [18].

the PSB, whereas in the EGM model, it was assumed that diffusional processes would be confined to narrow regions near the PSB-matrix interface, giving rise to ribbon-like extrusion growth at the interfaces [19]. The model of Brown [31] is similar in several respects to the EGM model but differs in important details, discussed in [13,18,19]. On the other hand, Brown analyzes the stress singularities at the PSB-matrix interface at the surface and the internal stresses induced by these dislocations and thus derives a crack initiation criterion. In the EGM model, stage I cracks are expected to initiate at the PSB-matrix interfaces. It is considered probable that these microcracks have in the past frequently been regarded as "intrusions". Crack initiation in the sharp valleys of the roughness profile appears also possible. The EGM model also explains the initiation of intergranular cracks at surface sites at which PSBs, with Burgers vector directed at the grain boundaries (GBs), impinge against the latter. Such PSB-GB cracks have been observed frequently and are dominant at low and intermediate amplitudes [30].

2.3.3. Experimental observations of PSB surface profiles: earlier studies and recent AFM observations

The main results of earlier work on fatigued copper single crystals by SEM surface observations [29,30] and studies of metallographic sections by high-resolution techniques such as the sharp corner technique [29] and modifications thereof [32] were as follows. In the early stages, extrusions of a bulgy form develop and grow. Only later, when the surface profile has become more complex, are intrusion-like deepenings observed. Extrusion-intrusion pairs are not found in representative numbers. In fatigued polycrystals, the extrusion heights are much smaller, and surface roughening which is sometimes more prominent is clearly documented [30]. An unexpected observation is the occasional occurrence of *isolated extrusions* [29,30,32,33]. Aside from the latter which is not understood, these earlier findings are broadly and semi-quantitatively in agreement with the EGM model. The main disagreement with the work of Polák and co-workers [27,28,33,34], see also their recent review article [35], concerns the frequency of occurrence of intrusions and their shape. In this respect, the quite recent high resolution observations of these authors with atomic force microscopy (AFM) are of particular interest [33,34]. A disadvantage is that this work was performed on polycrystalline material (stainless steel) with correspondingly smaller effects than would have been the case, had the work been done on single crystals or material with larger grain size. Figure 3 shows an example [33]. When the surface profile of extrusions/intrusions is probed, only the contours of the extrusions on the sides that make an obtuse angle with the surface are accessible to AFM (Fig. 4a), and narrow intrusions/cracks cannot be studied, because the AFM tip cannot enter into narrow valleys. Polák et al. [34] overcame these difficulties by studying replicas of the surface by AFM, as illustrated in Fig. 4b. Using this technique, they found surface profiles of the type indicated schematically in the figure, namely bulgy extrusions with an "intrusion" adjacent to it. However, these "intrusions" were much narrower than the extrusions, compare Fig. 4. Hence, it seems inappropriate to speak of extrusion-intrusion pairs. Rather, in the eyes of the author, these "intrusions" are more probably stage I shear cracks, formed in response to the formation of the extrusions, as proposed earlier [18,19].

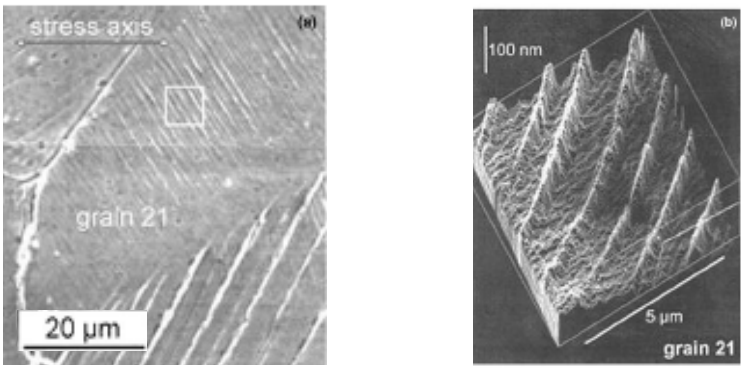

Fig. 3. AFM images of surface relief of fatigued austenitic stainless steel 316 L. a) Survey of different grains. b) Enlarged view of encircled area with extrusions in grain 21. From Man et al. [33]. Courtesy of the authors.

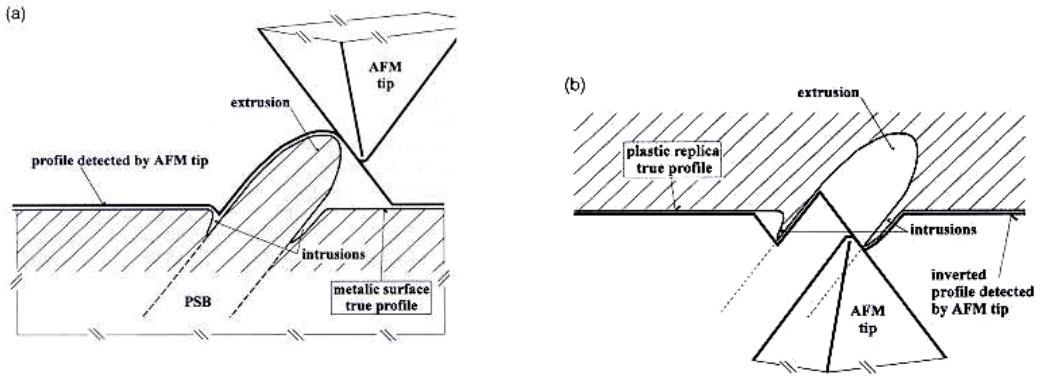

Fig. 4. Assessment of surface relief of fatigued metals by AFM. a) AFM of surface of fatigued specimen, detection of extrusions. b) AFM of surface replica of fatigued specimen, detection of "intrusions". After Polák et al. [34]. Courtesy of the authors.

3. Fatigue of ultrafine-grained (and nanocrystalline) metals

With the development of a number of so-called Severe Plastic Deformation (SPD) techniques, most notably Equal Channel Angular Pressing (ECAP), it has become possible to produce *bulk* materials with submicron grain sizes and with dimensions of some cm [36]. These materials are referred to as UltraFine-Grained (UFG) materials, as opposed to truly NanoCrystalline (NC) materials with grain sizes $D < 100$ nm which are produced by other means. The monotonic strength enhancement achieved by grain refinement follows from the well-known Hall-Petch relationship:

$$\sigma_y = \sigma_0 + k \cdot D^{-1/2}, \tag{4}$$

where σ_y is the yield stress, σ_o the friction stress, k a constant and D the grain size. The UFG microstructure after ECAP depends characteristically on the routes of ECAP processing (which specify how the billet is re-inserted into the ECAP die after each pass) [36,37]. Since NC materials are not available as readily in bulk form suitable for

standard mechanical testing as the UFG materials, most of the studies performed to date have been made on UFG materials prepared by ECAP processing. Still, some of the results obtained so far apply also to NC materials.

The considerable strength enhancement by a factor of up to about 4 that is achieved in UFG (and NC) materials as compared to materials of conventional grain (CG) size *(D* ≈ 10 μm or larger) has provided a strong incentive to develop UFG materials further for real engineering applications. Hence, the materials envisaged must have superior all-round mechanical properties, including in particular a very good fatigue resistance. It is gratifying to see that, in contrast to the focus of earlier work, there have been increasing studies of the fatigue properties in recent times, compare the reviews [38,39,40,41,42,43]. In the following, some of the main results achieved will be reviewed.

3.1. Grain-size dependence of cyclic deformation and fatigue behaviour - some basic considerations

The cyclic stress-strain behaviour of fcc and bcc metals of conventional grain size does not exhibit a marked grain-size dependence [44], aside from effects due, for example, to textures. In particular, the cyclic stress level of CG materials does not exhibit a Hall-Petch behaviour for different grain sizes as in the case of monotonic deformation. Nonetheless, the fatigue lives do vary more or less strongly with grain size, as documented, for example, for fcc metals like copper, aluminium and α-brass [45]. In CG materials, cyclic hardening and softening result from the accumulation and annihilation of dislocations, respectively, and characteristic dislocation bundles, tangles, cell walls, etc. form *within* the grains. As a consequence, the dislocations glide paths L are significantly smaller than the grain size ($L << D$) The characteristic microstructural spacings, e.g. the distances or cell sizes d from wall to wall, vary inversely with the stress level σ and follow a simple relationship of the form [46,47]

$$d = \frac{KGb}{\sigma}, \tag{5}$$

where G is the shear modulus and b the modulus of the Burgers vector. The constant K has a typical value of 10. If one now considers how small d can become for the highest possible stresses achieved in monotonic loading, one finds, for example, in the case of copper, that $d \approx 400$ nm represents a crude lower limit to the magnitude of the cell size [47]. Comparing this with the typical grain size of UFG copper of about 300 nm, it becomes evident that in UFG materials, and more so in true NC materials, the grain size is too small to allow the building-up of cell structures within the grains. Hence, cyclic hardening/softening as a consequence of the formation or rearrangement of a dislocation substructure within the grains can be excluded as a dominant mechanism [48,49], as illustrated in Fig. 5. In this grain-size range, the grain boundaries are the main obstacles to dislocation glide, and the glide paths now are of the order of the grain size ($L \leq D$!!). As a consequence, it is found that the grain boundary components of the cyclic stresses of UFG and C materials exhibit a grain-size dependence of a similar form as the Hall-Petch relationship, as shown for nickel in Fig. 6, see [48,49] for details.

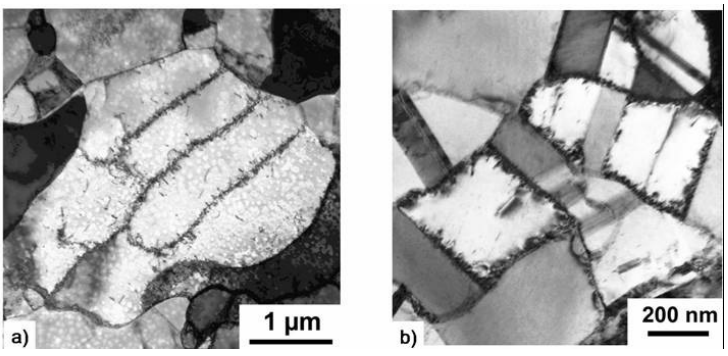

Fig. 5. TEM micrographs of dislocation microstructure in fatigued nickel specimens of different grain sizes. a) Fatigue-induced dislocation substructure inside the grains of specimen with larger grain size. b) Absence of fatigue-induced dislocation substructure inside the grains in specimen with very small grains. From [49]. Courtesy of the author.

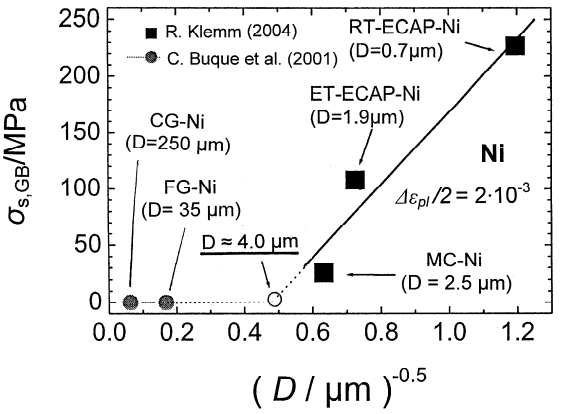

Fig. 6. Hall-Petch plot of grain boundary contribution $\sigma_{s,GB}$ to cyclic saturation stresses σ_s of nickel of different grain sizes D (FG: fine-grained, MC: microcrystalline, RT-ECAP and ET-ECAP refer to ECAP at room and at elevated temperature, respectively). The grain sizes are indicated in the figure. Adapted from Klemm [49]. With permission of the author.

3.2. Fatigue lives: comparison between UFG and CG materials

According to Morrow [50] and Landgraf [51], the Low Cycle Fatigue (LCF) life is controlled by fatigue ductility, whereas the High Cycle Fatigue (HCF) life is governed by the fatigue strength. This is expressed best in the total strain fatigue life diagram according to the relationships

$$\frac{\Delta\varepsilon_t}{2} = \frac{\Delta\varepsilon_{el}}{2} + \frac{\Delta\varepsilon_{pl}}{2} \tag{6}$$

$$\frac{\Delta\varepsilon_t}{2} = \frac{\sigma_f'}{E}(2N_f)^b + \varepsilon_f'(2N_f)^c \tag{7}$$

Here $\Delta\varepsilon_t$, $\Delta\varepsilon_{el}$ and $\Delta\varepsilon_{pl}$ are the total, the elastic and the plastic strain ranges (twice the amplitudes), respectively, N_f is the number of cycles to failure (2 N_f is number of load reversals to failure), E is Young's modulus, σ_f' is the fatigue strength coefficient, ε_f' the fatigue ductility coefficient, and b and c are the exponents of fatigue strength and

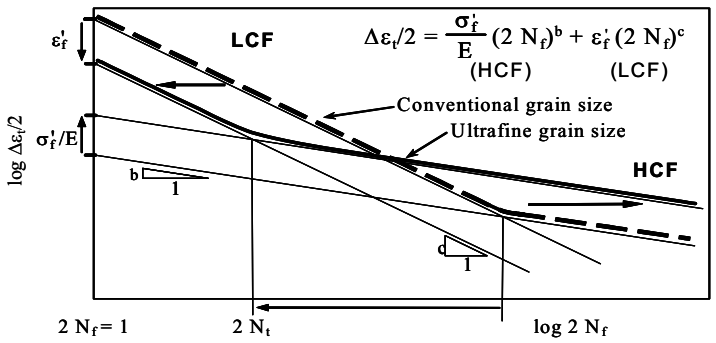

Fig. 7. Illustration of fatigue lives of strong UFG and more ductile CG materials in a total strain fatigue life diagram. After [38].

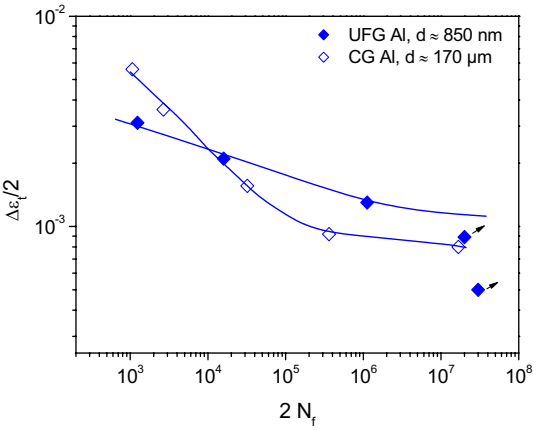

Fig. 8. Total strain fatigue life diagram showing the crossing of the fatigue life curves of UFG and CG aluminium. From [52,53].

ductility, respectively [50,51]. Equating the first terms of both equations, the well-known Basquin fatigue life law for the HCF regime is obtained, whereas equating the second terms of both equations leads to the equally well-known Coffin-Manson relationship for the LCF range. In the asymptotic limits of LCF ($\Delta\varepsilon_{el} << \Delta\varepsilon_{pl}$) and HCF ($\Delta\varepsilon_{el} >> \Delta\varepsilon_{pl}$), Eq. (7) reduces to the Coffin-Manson and the Basquin relationships, respectively. Since the UFG material exhibits the higher strength, compared to the CG material, whereas the latter has the larger ductility, the total strain fatigue life diagrams of UFG and CG materials can be constructed schematically, as proposed earlier [38] and as shown in Fig. 7. For $2N_f = 1$, the asymptotic Coffin-Manson and Basquin representations intercept the ordinate at ε_f' and σ_f'/E, respectively. Since ε_f' is larger for the CG than for the UFG material, whereas σ_f'/E is larger for the UFG than for the CG material, the two plots are expected to intersect. This has been found to be the case for copper, α-brass and aluminium [52,53]. As an example, the total strain fatigue life diagrams of UFG and CG aluminium of commercial purity are shown in Fig. 8. Some exceptions to this behaviour will be discussed later.

3.3. Summary of cyclic deformation behaviour and fatigue-induced microstructural changes and damage

The main results of the early observations which were made mainly on cyclically deformed UFG copper [38,48,54-59] and partly also on UFG nickel [58,59] can be summarized as follows:

- The cyclic stresses in strain-controlled tests were about 2 to 4 times larger than in similar tests on CG material.
- More or less severe *cyclic softening* was observed in strain-controlled tests [38,48,54-59], whereas there was almost no cyclic softening in stress-controlled tests [38,54,59].
- On the surface, cyclic strain localization in *macroscopic shear bands* (Figs. 9 a and 9b), extending over much larger distances than the UFG grain size, was observed. Fatigue cracks initiated in these shear bands [38,54-58].
- Inside the fatigued specimens, with a few exceptions, it was difficult to see marked changes of the microstructure related to the shear bands. However, there were patches of severely coarsened grains next to regions with the original UFG microstructure, i.e a *bimodal grain size distribution* had evolved, in particular during strain-controlled fatigue [48,49,54,58,59], as shown in (Fig. 9c), and less so in stress-controlled fatigue [38,58,59].
- As detailed elsewhere [42], both the grain coarsening and the shear banding observed are seen as the microstructural reasons for the cyclic softening.
- The fatigue lives of the UFG specimens were generally found to be larger than those of CG specimens in all Wöhler/S-N plots, but smaller, when the data were plotted in a Coffin-Manson diagram [38,54,57,58]. This finding agrees very nicely with the expectations according to the total strain fatigue life diagram shown in Fig. 7, UFG material showing larger lives than CG material in the HCF and shorter lives in the LCF range [38].

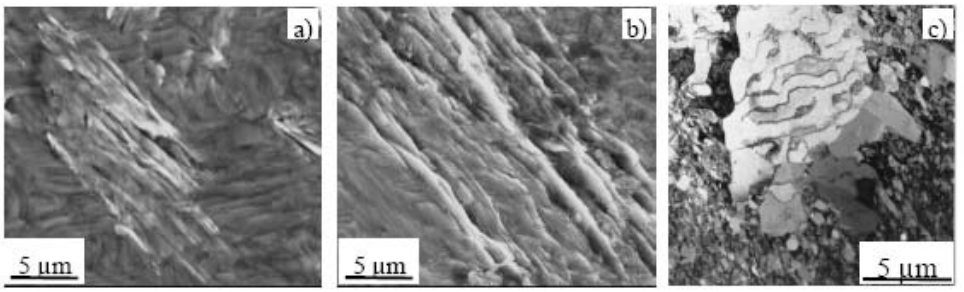

Fig. 9. Shear banding in UFG copper after strain-controlled fatigue at RT. Stress axis horizontal. Surface observations. a) Shear bands in "patches". b) Extended shear bands. c) TEM observation of locally coarsened grain/subgrain microstructure. After [38,58].

Since UFG materials produced by ECAP are heavily predeformed, the occurrence of microstructural instabilities which lead to grain coarsening and shear banding is not so surprising. In the case of UFG copper, it should be noted that grain coarsening was observed even at room temperature (RT), i.e. at a homologous temperature as low as 0.2 T_m (T_m: melting temperature), after mild cyclic strain-controlled deformation and was attributed to *dynamic recrystallization* [59]. Interestingly enough and not entirely understood, this type of fatigue-induced coarsening was almost absent in stress-controlled fatigue [38,59]. Furthermore, attention is drawn to the fact that dislocation patterns typical of fatigued CG materials developed in the coarser grains of the bimodal grain structure, as shown in Fig. 9c. In passing, it is noted that Witney et al. [60] were probably the first to observe cyclic strain localization in shear bands along the plane of maximum shear stress, accompanied by a modest increase of grain size, in some preliminary fatigue tests on nanocrystalline copper prepared by inert gas condensation ($D \approx 20$ nm). Both the bimodally coarsened grain structure and the shear bands result from fatigue-induced microstructural instabilities and are forms of *fatigue damage.* Hence, it is important to discuss in a little more detail their formation and properties. For a more through discussion, the reader is referred to a very recent review article [42].

The shear bands which represent sites of severe cyclic strain localization in which fatigue cracks initiate were originally observed to lie under an angle of approximately 45° to the stress axis, i.e. on the plane of maximum resolved shear stress [38,54,55,56,57,58]. The author had proposed two possible mechanisms of their formation, namely a) spreading of small regions of coarsened grain size into shear lamellae and/or b) the spreading of a microstructural instability caused by the change of strain path, when an ECAP-processed (sheared) material is subjected to a monotonic deformation [38]. So far, unequivocal evidence for either mechanism a) or b) is lacking. The observation of Wang et al. [61] that local recrystallization occurred first and in fact then lead to cyclic strain localization would favour mechanism a). Other authors have provided experimental evidence that sometimes the shear bands develop inside "precursor" shear bands that were formed along the shearing plane of the last ECAP pass [62-66]. This view seems to be justified in those cases in which the shear bands are inclined under an angle of approximately 26° to the stress axis, i.e. under the same angle under which shearing during ECAP occurs [66]. With a few exceptions, it has generally been found difficult to find by TEM (or SEM) marked microstructural evidence of the shear bands in the bulk. Thus, the Brno group [63,64,67] proposed that the shear bands are confined to the near-surface regions and that localized shear within the bands occurs by cooperative grain boundary sliding. However, some other studies on fatigued high-purity UFG copper with a grain size $D \approx 300$ nm [68], commercial purity UFG aluminium with grain size $D \approx 800$ nm [69] and more recently on commercial purity UFG aluminium with a grain size of $D \approx 590$ nm [70] have provided microstructural evidence that the shear bands are a bulk phenomenon. In more recent work on fatigued commercial-purity aluminium, clear TEM evidence of shear bands that could be clearly distinguished from the surrounding material and that contained a high density of dislocations was obtained. In spite of the not so different grain microstructure inside the shear bands, it could be shown that there was a loss of microhardness of about 20%, as compared to the adjacent material [70]. In UFG copper fatigued at -50°C, cyclic softening and grain coarsening were largely suppressed [38,58], indicating that cyclic softening is at least partly a thermally activated process. In summary, the bulk of the evidence suggests that *both* grain coarsening by dynamic recrystallization and macroscopic shear banding are responsible for cyclic softening.

Dynamic recrystallization requires easy grain boundary motion. Hence, less pure UFG materials with reduced grain boundary mobility are expected to exhibit better microstructural stability. Thus, the finding by the Brno group that grain coarsening was not observed in fatigued commercial-purity copper seemed to be in line with this expectation [63,64]. However, since all the fatigue tests by the Brno group had been performed in stress and not in strain control, an uncertainty remained, which was only resolved in very recent work of the Brno group. In these studies, strain-controlled tests were conducted on commercial purity copper at RT, and similar cyclic softening and bimodal grain coarsening, as observed earlier on pure UFG copper [71], were found, indicating that, at least at RT, UFG copper does not exhibit a marked impurity effect. In this context, results obtained on cyclically deformed UFG copper produced by a non-standard ECAP route (16E) are of interest [72]. The UFG copper, although of high purity, was found to be cyclically stable at RT in strain-controlled fatigue. The additional observation that the hysteresis loops displayed nearly perfect Masing behaviour also indicated good cyclic stability of the microstructure. This discussion illustrates that several factors must be considered when discussing the microstructural stability of UFG copper and other pure materials. It is of interest that, in the case of (commercial purity) structural UFG materials, rather good microstructural stability has generally been found [39,41,42].

Some instructive fatigue life data of UFG copper from the work of the Brno group [67,73] are shown in Figs. 10a and 10b. It should be noted that the fatigue life data shown in Fig. 10 extend into the regime of so-called Ultrahigh or Very High Cycle Fatigue (UHCF, VHCF) with numbers of cycles to failure N_f in excess of 10^9. In this extensive study, the influence of purity and ECAP routes (B_c and C) on the stress-controlled fatigue behaviour were studied for three purity grades: 99.5%, 99.8% and 99.998%. In the Wöhler (S-N) plot, Fig. 10a, a strong effect of purity, showing that the fatigue strength of high-purity copper is inferior to that of less pure copper, is found and also a strong effect of the ECAP route: specimens 99998/B_c/6 exhibit shorter fatigue lives than specimens 99.998/C/6. When the fatigue life behaviour is plotted in a Coffin-Manson plot (Fig. 11b), it is interesting to note that all data, irrespective of purity and ECAP route fall into a narrow band. This led the authors to conclude that the plastic strain amplitude is a "unifying parameter" with respect to life-time prediction. The same authors also performed a thorough study of the effects of temperature on fatigue life and on the CSS behaviour of UFG copper in the range between 103 K and room temperature [67,73]. One very interesting result was that the CSS curve of UFG copper shows only a rather small dependence on temperature, in strong contrast to the CSS curve of CG copper. This finding is an indication that the strength of UFG materials is governed much more by the grain boundaries than by dislocation distributions inside the grains.

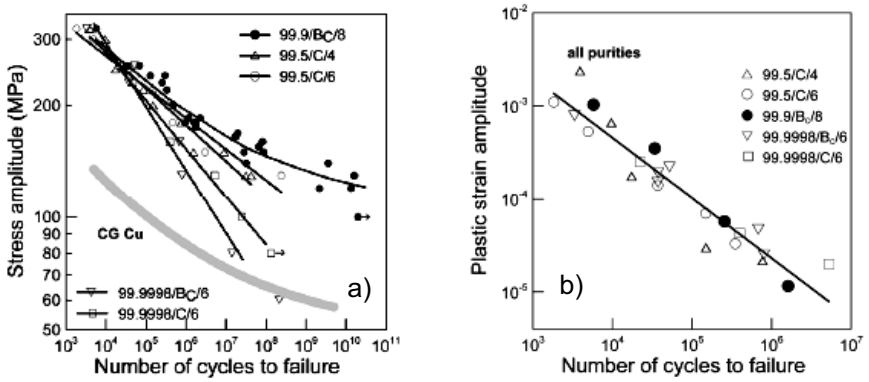

Fig. 10. Fatigue life curves of UFG copper of different purities and of CG copper. a) Wöhler (S-N) representation, showing the strong dependence of the fatigue lives of UFG copper on purity, in particular in the HCF and UHCF ranges. b) Coffin-Manson representation, almost collapse of data of UFG copper of different purities. Specimen designations refer to purity/ECAP route/number of ECAP passes. From [67,73]. Courtesy of the authors. With permission.

3.4. Enhanced fatigue resistance of annealed bimodally grain coarsened UFG materials

In early work on UFG copper fatigued in strain control, it had been noted that, in a Coffin-Manson plot, the LCF fatigue lives of UFG material were shorter than those of CG material [38,54,57,58], in conformity with Fig. 7. In order to improve the LCF fatigue behaviour, the UFG material was annealed mildly with the aim to enhance the ductility at the expense of a moderate loss of strength [38,58,74]. Thereupon, a bimodally coarsened grain structure was formed which looked similar to that observed after strain-controlled fatigue. The fatigue lives of UFG specimens containing this bimodal grain structure were significantly larger (by a factor of 7) than those of unannealed UFG material. This suggested that the introduction of a bimodal grain structure could be a general measure to markedly improve the overall mechanical properties of UFG materials, as had also been advocated subsequently in the case of monotonic deformation [75]. However, so far, it has not been possible to achieve similarly large enhancements of fatigue performance in UFG materials other than UFG copper [40,41,42].

In the case of ECAP-processed UFG copper, a detailed assessment of the evolution and effects of bimodally coarsened UFG grain structure has been made [76], and some new fatigue life data of UFG copper produced by ECAP without and with back pressure (BP) was presented and compared with the fatigue lives of CG copper. Very surprisingly, the microstructures of both batches of ECAP-processed copper were found to be bimodally coarsened shortly after ECAP. The reasons are still not quite clear. The fatigue life data of the ECAP-processed copper data and of the CG counterparts, supplemented with CG data from an earlier study [44], are shown in a total strain fatigue life plot in Fig. 11. Within the scatter, the fatigue lives of the copper specimens that had been ECAP-processed with or without back pressure were similar. The same was true for the two sets of CG data. Hence, all ECAP/bimodal and all CG data were lumped together. By fitting the two sets of data to the total strain fatigue life relationship according to Eq. (7), the relevant constants σ_f', ε_f', b and c were obtained for both sets of data. Using these values, the total strain fatigue life curves were computed according to Eq. (7) and plotted in the figure. The interesting result is that, over the whole life range investigated, the bimodally coarsened UFG copper exhibited markedly longer fatigue lives than the CG copper. This result confirms the beneficial effect of bimodal grain coarsening in the case of copper. Beyond that, the result is reminiscent, with respect to fatigue, of what Valiev referred to as the *"Paradox of strength and ductility in metals processed by severe plastic deformation"* [77], implying that, in severely plastically deformed metals, both the strength and the ductility can be enhanced. The impressive results shown here for fatigued ECAP-processed copper, with superior fatigue resistance in LCF and HCF, come close to the case of Valiev's paradoxon.

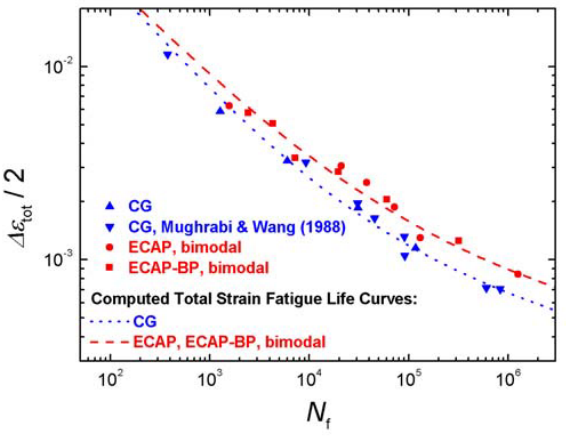

Fig. 11. Total strain fatigue life data of bimodally coarsened ECAP-processed copper (with and without BP), comparison with data of CG copper. Based on fatigue life data of [76]. See text for details.

3.5. Enhanced fatigue crack growth in UFG and NC materials

Frequently, fatigue cracks in UFG materials initiate in the fatigue-induced shear bands. In stress-controlled HCF tests, very fine-grained materials (UFG and NC) always exhibit larger fatigue lives and a higher endurance limit than CG materials, indicating that grain refinement enhances the resistance against crack initiation. With regard to crack initiation, it is noteworthy that UFG copper has been shown to be more notch-sensitive than CG copper [78]. In the same study, it was found that, within the plastic zone, the grain structure differed from that of neighbouring regions, the grains being more elongated. Since the total fatigue life is made up of the cycles spent during crack initiation and during crack propagation, the problem of fatigue crack growth has been addressed in several fracture mechanics studies on different UFG (and NC) materials and their CG counterparts [39,79,80,81]. As summarized in [42], broadly similar results were obtained by different authors, for example, on different very fine-grained (NC or UFG) metals and alloys and their CG counterparts, namely on nickel, titanium, aluminium alloys, aluminium, copper and titanium and a low carbon steel. The main result was that, with increasing grain refinement, the fatigue crack thresholds were lowered and the fatigue crack growth rates were enhanced. These findings were attributed to the smoother fracture paths and reduced crack closure for the smaller grain sizes. Furthermore, a Hall-Petch dependence on grain size was noted for both the fatigue endurance limit and the threshold stress intensity range [39].

3.6. Fatigue lives of some UFG structural materials,

The work discussed in the preceding sections related mainly to basic studies on simple materials that permitted to obtain some insight into the basic mechanisms of cyclic deformation and fatigue of very fine-grained materials. More recently, attention has been focused also on structural materials which could potentially be used in practical applications. Most of the work was done on light metal UFG aluminium, titanium and magnesium alloys, compare the reviews [39,40,41,42,82]. In addition, a limited amount of work has been performed on UFG steels, see for example [42,83,84]. Here, we address only a few special cases. Recent studies of the fatigue behaviour of Al-Mg by May yielded interesting results on the effects of Mg content, ECAP route and number of ECAP passes [85]. In particular, the microstructural stability was enhanced by the Mg content and the number of ECAP passes. Also, in all cases, the total strain fatigue life curves of UFG and CG material intersected, as expected on the basis of Fig. 7.

In earlier work, the fatigue of UFG titanium [39,86] was studied. More recent work [87] dealt with the fatigue properties of the important titanium alloy Ti-6Al-4V ELI (extra low interstitial). Fatigue life data of UFG and CG material of this alloy are shown in Figs. 12a and 12b. The Wöhler (S-N) plots (Fig. 12a) show a very strong improvement of the fatigue properties by grain refinement for the two UFG conditions investigated (UFG1: 2 ECAP passes, B_c; UFG2: 4 ECAP passes, B_c). (The additional CG data shown for comparison are from other work using rotating-bending tests with R ratio zero, see [87].) In Fig. 12b, the total strain fatigue life data, resolved into the Coffin-Manson ($\Delta\varepsilon_{pl}/2$ vs. N_f) and Basquin ($\Delta\varepsilon_{el}/2$ vs. N_f) parts, are shown. As expected, the Coffin-Manson plot of the CG material (with a change of slope which is typical of the material [87]) shows longer fatigue lives than that of the UFG material, and the Basquin data show an improvement of the UFG material compared to the CG material. Nevertheless, it should be noted that, in contrast to the cases discussed earlier, the fatigue life curves of UFG and CG material do not cross.

Turning to UFG steels, Fig. 13 from the work of Furuya et al. [88] compares in a plot of the fatigue limits against the tensile strengths the behaviour of UFG ferrite-cementite steels and conventional tempered martensite and ferrite-pearlite steels. In this case, the UFG material had not been produced by ECAP but by "multipass warm caliber rolling". The fatigue tests were performed at RT in rotating bending [88]. The authors concluded that "the fatigue strength of the UFG ferrite-cementite steel matched that of the tempered martensite steel". This result is in line with the findings discussed above for other materials, namely that the HCF fatigue strength of UFG materials is in general superior to that of the CG material counterparts. Quite different very elaborate studies were conducted by the group of Maier which studied in particular the RT LCF behaviour of UFG interstitial-free (IF) steels that had been produced by different numbers of ECAP passes, using a variety of ECAP routes. As for UFG copper, aluminium and α-brass, it was found that, in a Coffin-Manson plot, the UFG IF steels investigated showed a shorter fatígue life than the CG IF steel [89]. While these results are in line with the concepts on which Fig. 7 is based, it is noted that so far there exist no data on the fatigue lives over a large range from LCF to HCF of UFG and CG specimens of one and the same UFG steel.

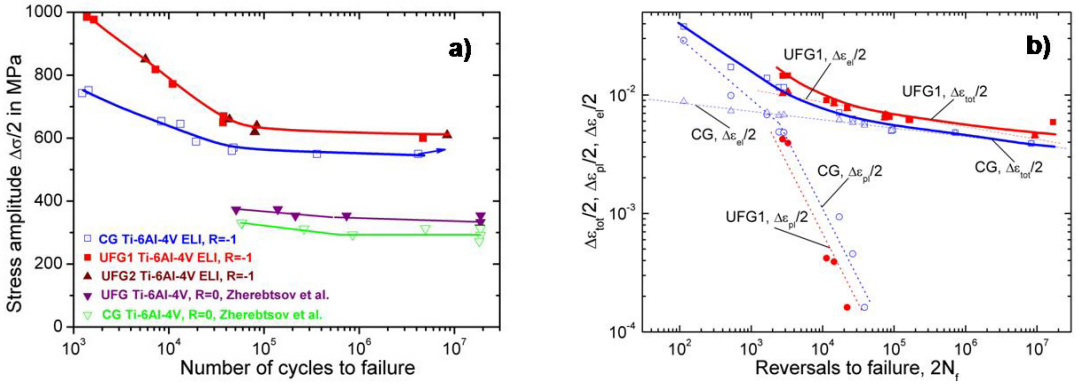

Fig. 12. Fatigue lives of two UFG variants of alloy Ti-6Al-4V ELI, comparison with CG alloy. a) Wöhler (S-N) plots, UFG alloys show enhanced fatigue strength. b) Total strain fatigue life plots, UFG materials, especially UFG 1, show improved fatigue performance over the whole range. From [87]. With permission.

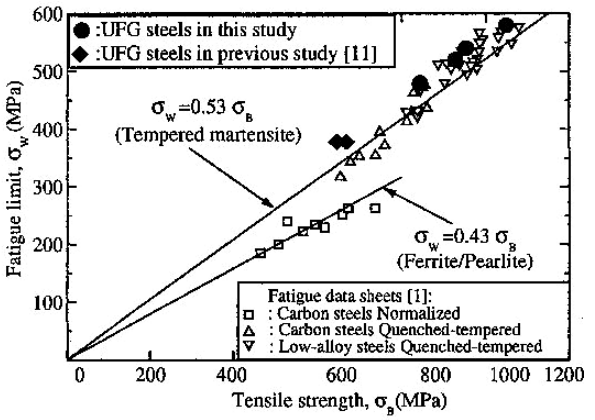

Fig. 13. Comparison of fatigue limits of UFG and some CG steels as a function of tensile strength. After [88]. With permission.

4. Ultrahigh cycle fatigue (UHCF)

4.1. Background of the Gigacycle or UHCF problem

In standard laboratory fatigue tests, the number of cycles is usually limited to about 10^7. On the other hand, there are many examples of failures in practice after much larger numbers of cycles, with N_f in the range of 10^9 or higher. Such failures occur commonly in vibrating or rotating machine components, e.g. in pumps, combustion engine cylinders or also in roller bearings and axles of high-speed trains. Only after Claude Bathias and Stefanie Stanzl-Tschegg had organized the International Conference "Fatigue Life in Gigacycle Regime" (later called VHCF-1) in the year 1998 [90], has this field become an important part of basic fatigue research. Nowadays, this topic is named Ultra High Cycle Fatigue (UHCF) or Very High Cycle Fatigue (VHCF). Here, as in earlier publications [91,92,93],

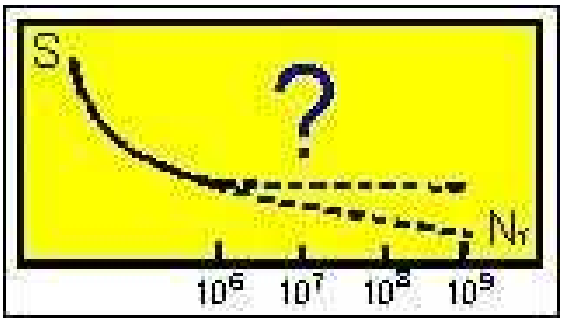

Fig. 14. Schematic Wöhler diagram, emblem of the conference "Fatigue Life in Gigacycle Regime" (VHCF-1), with indication of uncertainty regarding the existence of a fatigue limit in the UHCF regime. Courtesy of C. Bathias.

the author will use the term UHCF. Fig. 14 shows the emblem selected by Claude Bathias for the announcement of the conference VHCF-1. It illustrates an example of a Wöhler/S-N diagram which is considered suitable to characterize the key problem of this topic. In Fig. 14, the stress amplitude S is plotted on the ordinate and the number of cycles N_r to failure (r: rompu. French for ruptured) on the abscissa. As expected intuitively, the fatigue lives are the larger, the lower the stress amplitude is. Above 10^6 cycles, two possible courses of the Wöhler plot are indicated and marked with a big question mark. The horizontal course would imply that a fatigue limit exists, whereas in the case of the continuously slanting course, fatigue failures would occur also at increasingly lower stress amplitudes, though of course after longer fatigue lives. This is the problem at the heart of UHCF. Based on general experience, the author has always emphasized that, at very long fatigue lives, typical of very low loading amplitudes at which only very few grains deform plastically, crack initiation rather than propagation will be life-governing, unless crack propagation occurs early at pre-existing sites of damage [91,92,93].

In view of the large numbers of cycles, UHCF studies are frequently conducted with ultrasonic testing techniques at frequencies of about 20 kHz, compare [94]. Early UHCF research focused primarily on high-strength steels which frequently exhibit subsurface so-called fish-eye failure at heterogeneities such as, in particular, non-metallic inclusions of ca. 10 µm diameter [95,96,97,98]. In the following, the current knowledge on UHCF behaviour will be summarized with reference to simple ductile fcc metals like copper or nickel, on the one hand, and high-strength steels, on the other hand. In order to distinguish these very different materials, the author has called the former Type I materials and the latter Type II materials [92,93]. Here, the following aspects will be presented and discussed, first for Type II, then for Type I materials:

- Fatigue life diagrams extending into the UHCF regime
- Microstructural failure mechanisms and life-governing factors

4.2. Type II materials: Fatigue life plots, surface and subsurface failures.

The main results of the work of the research groups of Murakami [95], Bathias [96], Sakai [97] and Nishijima and Kanazawa [98] on UHCF of high-strength steels (as typical Type II materials) are as follows. A fatigue limit is found above about 10^4 cycles. However, this fatigue limit extends only up to less than 10^7 cycles, and at higher numbers of cycles, fatigue failures are observed to occur at stress levels below this fatigue limit! Furthermore, within statistical scatter, it is found that at stress levels above the fatigue limit, surface failures are dominant, whereas at lower stress levels, subsurface internal failures in the form of so-called "*fish-eye fractures*", originating from subsurface inclusions, occur predominantly. In summary, the fatigue lives of high-strength steels as typical Type II materials can be represented schematically over the whole range, from LCF to UHCF, as shown in Fig. 15. Since the plastic strain amplitude $\Delta\varepsilon_{pl}/2$ or the stress amplitude $\Delta\sigma/2$ are mutually convertible via the CSS curve [99], this schematic fatigue life diagram can be viewed as a Wöhler/S-N or a Coffin-Manson plot, depending on whether $\Delta\varepsilon_{pl}/2$ or $\Delta\sigma/2$ are plotted on the ordinate. Approximate boundaries are indicated which separate the ranges

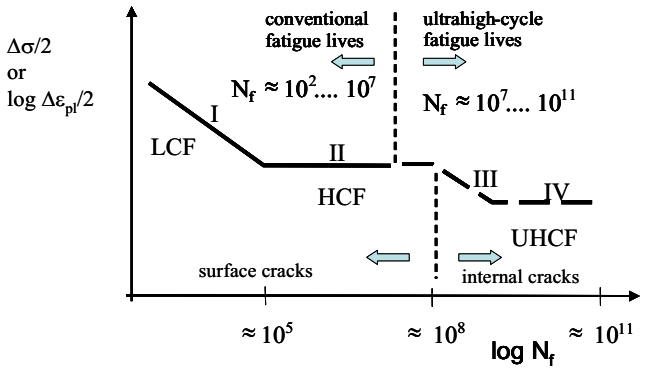

Fig. 15. Schematic multistage fatigue life diagram of Type II materials, with the ranges I, II, III and IV, corresponding to the LCF, HCF, HCF-UHCF transition and UHCF ranges, respectively. After [93].

of HCF and UHCF, on the one hand, and surface and subsurface internal failures on the other hand. Bathias [100] has explained schematically how the crack initiation frequency and sites vary, as one goes from LCF to HCF and then to UHCF:

- In the LCF range, at fairly large stress amplitudes, many crack initiation sites develop at the surface for different reasons (surface roughening, grain shape changes, slip bands, etc.).
- In the HCF regime, at somewhat lower stress levels, surface damage still occurs but in a less severe manner. Thus the crack initiation sites are of similar type but less severe, and they occur in smaller numbers.
- Finally, in the UHCF range, at even smaller stress amplitudes, surface damage becomes more or less negligibly small. However, in high-strength steels containing internal heterogeneities such as in particular inclusions, internal cracks can initiate at these inclusions. This probably occurs also in LCF and HCF but remains "unnoticed", because of early surface failure. In UHCF, however, these cracks can propagate very slowly in vacuum!) from the interior to the surface and, in the end, cause internal failure.

Such dual-slope fatigue or multistage fatigue life behaviour has been found in particular for rotating bending fatigue [97] but only in special cases also for axial fatigue loading. Thus, Furuya et al. also reported dual-slope fatigue life behaviour in axial loading in the case of some steels but not in the case of other steels and argued that this depends on the size and type of the inclusions [101]. The available data do not permit to conclude whether, in range IV, an "ultimate" fatigue limit exists beyond $N_f \approx 10^9$ cycles. *Thus, the question whether such an ultimate fatigue limit exists in the UHCF regime remains questionable.* In very detailed studies on the UHCF behaviour of high-strength steels, Murakami and co-workers [95] analyzed carefully the details of fish-eye failures and emphasized that, at the origin of the cracks at inclusions, there is an "optically dark area" (ODA), in which slow crack growth assisted by hydrogen occurs up till the critical size of the ODA is reached, before normal crack growth takes over. In addition, they provided a simple relation (the "√<area>" parameter model") which describes the UHCF fatigue limit in terms of Vickers hardness and internal defect size related to the ODA. Other details of UHCF of steels are as follows:

- Big inclusions are more dangerous than smaller ones. Thus, big extrusions lying at greater depths can be more life-determining than smaller ones lying closer to the surface.
- The smaller the volume density of the inclusions, the less probable surface failures at inclusions will be. In fact, a critical inclusion density can be defined, below which surface failures at inclusions are very improbable [92].
- The author has proposed that fatigue crack initiation, including very slow early crack growth, very probably occupies a major portion of UHCF fatigue life [92,93]. Recent support for this view comes from work by the groups of Bathias and Paris [102]. The problem is the definition of the transition between crack initiation and propagation. One possibility is to define the regime of crack initiation up to that stage beyond which crack propagation can be described by linear elastic fracture mechanics [93].
- Surface roughness reduces fatigue life.

4.3. Type I materials: Fatigue crack initiation below the PSB threshold, fatigue crack initiation/life plots

In HCF of ductile fcc Type I materials, persistent slip bands (PSBs) are the most common form of fatigue damage. PSBs develop only, when the loading amplitude exceeds a well-defined critical threshold amplitude [17]. Considering that the number of cycles in the UHCF range is much larger than in the HCF regime, the question now is: Can fatigue damage develop in UHCF *even at amplitudes below the PSB thresholds,* and if so, in which form? In dealing with this question, the author has proposed a model [92,93] which is based on the following considerations:

- During cyclic deformation, the dislocation bundle/vein matrix structure is formed at first.
- The cyclic deformation in the matrix is not completely reversible but retains a very small irreversible component.
- As a consequence of the very high numbers of cycles, the only slightly irreversible glide processes eventually lead in a statistical manner to an accumulation of slip steps at the surface which give rise to an increasing roughening of the surface.
- With increasing surface roughness, local stress concentrations which develop in the valleys of the roughness can become so large that the PSB thresholds of the HCF range are exceeded *locally*, although the loading amplitudes lie below the PSB thresholds.
- Thus, PSBs can develop locally at these sites of high stress concentration and can possibly lead to the initiation of fatigue cracks.

This model of fatigue crack initiation below the traditional PSB thresholds under conditions of UHCF at very large numbers of cycles leads to a modified fatigue life diagram, shown schematically in a Coffin-Manson plot in Fig. 16 in which the plastic strain amplitude $\Delta\varepsilon_{pl}/2$ ($\Delta\varepsilon_{pl}$: plastic strain range) is plotted against the number of cycles to failure N_f . Since it is known that the loading amplitudes that are necessary in order to make cracks propagate are somewhat higher than those required for crack initiation [103], the HCF range and the UHCF ranges III/IV of the diagram refer, strictly speaking, not to the number of cycles to failure but only to the number of cycles to fatigue crack initiation. Range I in the figure corresponds to the well-known Low Cycle Fatigue (LCF) regime according to the Coffin-Manson law, and the plateau range II is defined by the traditional PSB threshold. The slanting slope of the plot in range III follows from the prediction that crack initiation is considered possible in the UHCF range even below the traditional PSB threshold, provided that the number of cycles is very large. Whether, in the approach to completely reversible dislocation glide in range IV, there exists an absolute fatigue limit, is an open question, just as in the case of Type II materials. An example of a fatigue life diagram showing some similarity to the proposed diagram is shown in Fig. 15 from the work of Höppel et al. on UFG aluminium [104]. In this case, the subtle details of the UFG data are probably brought out mainly because of the markedly enhanced stress level of the UFG material with respect to that of the CG material.

The question whether fatigue crack initiation in UHCF can occur below the PSB threshold was studied experimentally as follows. Polycrystalline copper polycrystals were fatigued ultrasonically up to more than 10^{10} cycles at amplitudes lying somewhat below the conventional PSB thresholds of the HCF regime [105,106,107]. Microscopic investigations were performed on the surface and on sections cut parallel to the specimen axis. In the latter case, in order to delineate the surface profile, the surface was either electrocoated with a copper layer or, in the

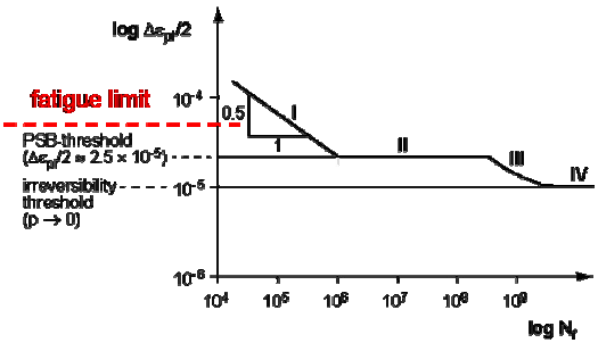

Fig. 16. Schematic multistage fatigue life diagram for type I materials (copper). After [91,106]

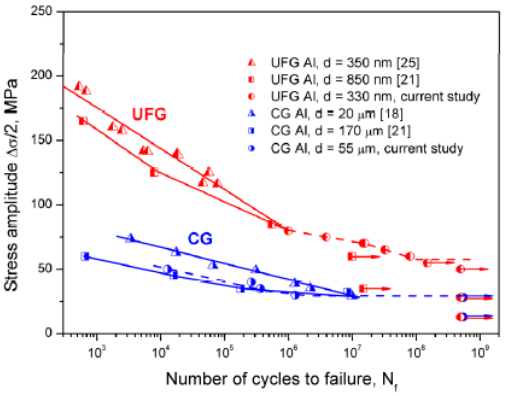

Fig. 17. Wöhler plot of ultrafine-grained aluminium (and CG aluminium of conventional grain size), with an indication of a second sloping off of the curve in the UHCF regime. Data of different authors. From Höppel et al. [104]. Courtesy of the authors.

case of studies using the FIB (focused ion beam) technique, a thin platinum layer was deposited on the surface before sectioning. The observations revealed, even after fatigue at amplitudes below the PSB thresholds, slip bands at the surface and a roughening of the surface with extrusions and so-called stage I shear cracks, as shown in Fig. 18. The surface roughening is seen more clearly at higher magnification in Fig. 18b. Figure 19a shows another view of the surface roughening with the stage I shear cracks which were better recognizable with secondary electron imaging (Figure 19b). The lamellar cyclic strain localization, as observed with electron channeling contrast (ECC) in the SEM using a backscattered electron detector, is shown in Fig. 19a. As expected, both the lamellar shear bands and the stage I cracks are aligned roughly under 45° to the stress axis, i.e. along the plane of maximum resolved shear stress. It is important to note that the stage I shear cracks were observed not only at the surface but also at greater depths, as discussed in more detail in ref. [107]. Aside from details, see [107], the main model predictions could thus be confirmed. Assuming that the surface roughness stems from random glide processes of unknown irreversibility p, it can be evaluated more quantitatively by making use of Equation (2). From the ultrasonic fatigue tests [105,106,107,108], the values for N (1.59×10^{10} cycles) and $\gamma_{pl,PSB}$ (1.37×10^{-5}) are known. In the latter case, it was assumed that $\gamma_{pl,PSB}$ corresponds to the PSB threshold value of the plastic shear strain amplitude at ultrasonic fatigue [108]. From the evaluation of the roughness profile (Figure 18b) for h = 2 μm, one obtains a value of $\overline{w} \approx$ 150 nm. Thus, all quantities in Equation (1) with the exception of the usually unknown glide irreversibility p are known. Hence, p can be determined. One then obtains the very small value $p \approx 0.000034$. However, since N is very large, the cumulative irreversible shear strain $\gamma_{pl,irr,cum}$ is nonetheless found to be very large, see Table 1, namely:

$$\gamma_{pl,irr,cum} = 4\,N \times p \times \gamma_{pl,PSB} \approx 34. \tag{8}$$

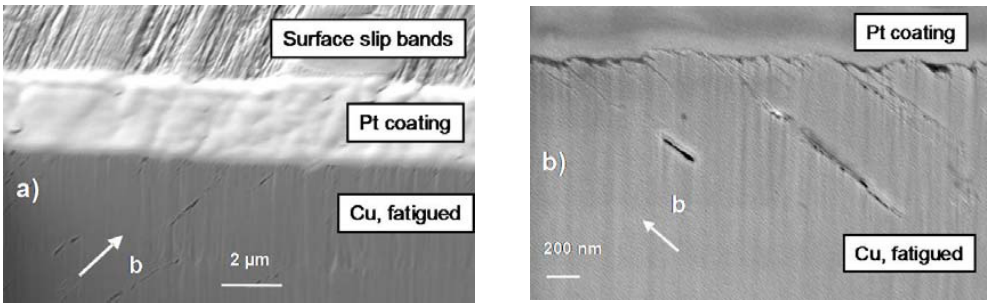

Fig. 18. FIB sections. a) Slip bands at the surface bounding FIB cut, showing surface roughening at the interface between Pt coating and fatigued copper and family of stage I shear cracks. b) Higher magnification of surface roughening, stage I shear cracks. After [107].

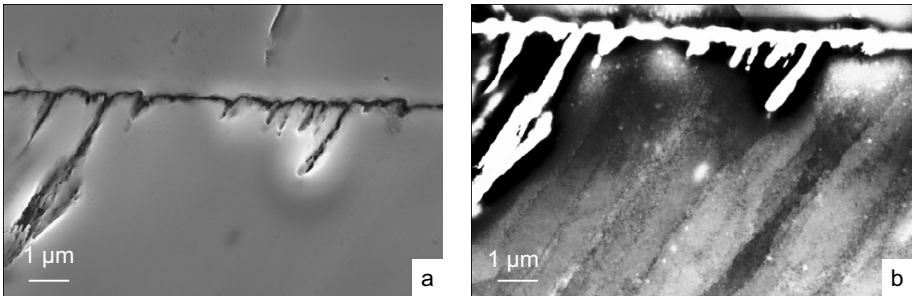

Fig. 19. Surface roughening, strain localization and stage I shear cracks in polycrystalline copper fatigued to 1.59×10^{10} cycles below the traditional HCF PSB threshold. a) Scanning electron micrograph, backscattered electron detector. b) Scanning electron micrograph, In-Lens secondary electron detector. Same area as in a).The specimen axis is horizontal. After [107].

It follows that, because of the very high cumulative irreversible shear strain, and in spite of the very small glide irreversibility *p*, very marked microstructural changes and fatigue damage can be expected to develop, as has indeed been observed experimentally. The question whether the stage I microcracks observed would lead to failure after fatiguing for still higher numbers of cycles remains open. Because of the limited experimental data in the regime of very high numbers of cycles, it is not possible to conclude reliably whether these cracks are able to propagate [107].

4.4. Conclusions with respect to the existence of a true fatigue limit: the Design Wöhler curve

There can be no doubt that the current research efforts in the UHCF field, as reflected in the series of Very High Cycle Fatigue conferences VHCF-1 to VHCF-4, held in the last decade, have brought to light many interesting aspects of UHCF and have furthered the fundamental understanding. Thus, it can be expected that in the near future UHCF problems will be well understood. One main result is emphasized. It now seems quite certain that, *for both Type I and II materials, albeit for different reasons, the traditional HCF fatigue limit does not extend into the UHCF regime.* Moreover, it is questionable whether an ultimate UHCF fatigue limit exists which would lie well below the traditional HCF fatigue limit. Motivated by these facts, Sonsino surveyed a large body of fatigue data extending beyond the HCF regime. He concluded that, for design purposes, a fatigue limit does not exist and recommended for practical purposes the modified fatigue life diagram shown in Figure 20 [109]. Sonsino calls this fatigue life diagram a "Design" Wöhler curve. For realistic technological cases, the pertinent fatigue life curve has no true (fictive) UHCF fatigue limit but, instead, a "knee point" beyond which the curve follows a slanting course. Thus, the fatigue lives increase but remain finite, as the stress amplitude decreases. Based on a detailed analysis of fatigue life data of different materials, Sonsino recommends appropriate knee points and slopes of the curves beyond the knee point.

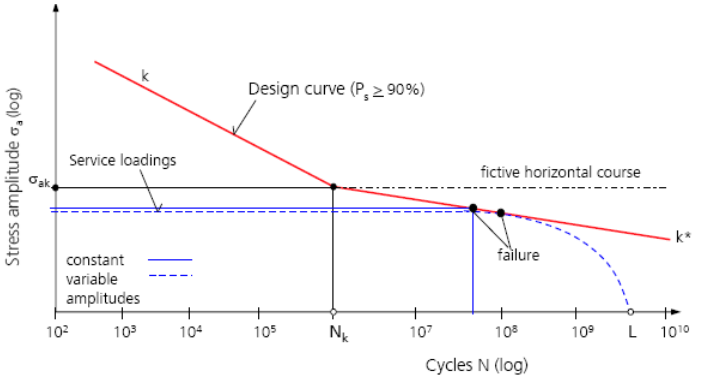

Fig. 20. Sonsino's "Design Wöhler curve" with no fatigue limit. After [109]. With permission.

5. Concluding remarks

The primary motivation for fatigue research is to understand how fatigue damage evolves under specific conditions of cyclic loading and ultimately causes failures. Based thereupon, strategies to improve the fatigue resistance can be devised. Ultimately, progress in these areas depends on achieving a deeper understanding of the microstructural mechanisms of cyclic deformation. In this sense, it is hoped that the examples discussed have illustrated the importance of basic studies on fatigue mechanisms with the goal to achieve technological advances.

References

[1] Blom AF, Ritchie RO. In Memoriam of Jim Beevers. In: Bailon JP, Dickson JI, editors. *Proceedings of the Fifth Interational Conference on Fatigue and Fatigue Thresholds (FATIGUE 93)*, Volume I, West Midlands: EMAS; 1993.

[2] Feltner CE, Laird, C. Cyclic stress-strain response of F.C.C. metals and alloys. Parts I and II. *Acta metall* 1967;15:1621-1632 and 1967;15:1633-1653.

[3] Feltner CE, Laird, C. The role of slip character in steady state cyclic stress-strain behavior. *Trans. TMS-AIME*, 1969;**245**:1372-73.

[4] Lukáš P, Klesnil M. Dislocation structures in fatigued single crystals of Cu-Zn system. *phys stat. sol. (a)* 1971;**5**:247-258.

[5] Mughrabi H. Mikrostrukturelle Ursachen der Ermüdungsrißbildung. In: Munz D, editor. *Ermüdungsverhalten metallischer Werkstoffe, Symposium der Deutschen Gesellschaft für Metallkunde*, Bad Nauheim, 1984, DGM Informationsgesellschaft Verlag;1985, p. 7-38.

[6] Mughrabi H, Wang R. Cyclic strain localization and fatigue crack initiation in persistent slip bands in single-phase metals and alloys. In: Sih GC, Zorski H, editors. *Proceedings of First International Symposium on Defects and Fracture*, Tuczno, Poland, 13th - 17th Oct. 1980, The Hague, Boston & London: Martinus Njihoff Publishers; 1982, p. 15-28.

[7] Karnthaler HP, Schügerl B. Dislocation structures in plastically deformed, disordered Ni_3Fe. In: Haasen P, Gerold V, Kostorz G, editors. *Proceedings of 5th Int Conf on the Strength of Metals and Alloys (ICSMA 5)*, Vol 1, Oxford: Pergamon Press; 1979, p. 205-210.

[8] Steffens Th, Schwink Ch, Korner A,Karnthaler HP. Transmission Electron Microscopy Study of Stacking-Fault Energy and Dislocation Structure in CuMn Alloys. *Phil Mag A* 1987;**56**:161-173.

[9] Clément N. Influence de l'ordre a courte distance sur les méchanismes de déformation des solutions solides. In : *L'Ordre et le Désordre dans les Matériaux,* Ecole d'hiver Aussois. Les Éditions de Physique;1984, p. 167-182.

[10] Gerold V, Karnthaler HP. On the origin of planar slip in fcc alloys. *Acta metall* 1989;**37**:177-2183.

[11] Berns H, Gavriljuk VG, Nabiran N, Petrov YuN, Riedner S, Trophimova LN. Fatigue and structural changes of high interstitial austenitic steels. *steel research international*, DOI: 10.1002/srin.200900142, in press.

[12] Ewing A , Humfrey JCW. The fracture of metals under repeated alterations of stress. *Phil Trans R Soc Lond A* 1903;**200**:241-250.

[13] Mughrabi H. Cyclic slip irreversibilities and the evolution of fatigue damage. *Metall and Mater Transactions A* 2009;**40**:1257-1279.

[14] Sommer C, Mughrabi H, Lochner D. Influence of temperature and carbon content on the cyclic deformation behaviour of α-iron; Part I: Cyclic deformation and stress-strain behaviour. *Acta mater* 1998;**46**:1527-1536.

[15] Thompson N, Wadsworth NJ, Louat N. The origin of fatigue fracture in copper. *Phil Mag* 1956;**1**:113-126.

[16] Lukáš P, Kunz L. Role of persistent slip bands in fatigue. *Phil Mag* 2004;**84**:317-330.

[17] Mughrabi H, Ackermann F, Herz K Persistent slip bands in fatigued face-centered and body-centred cubic metals. In: Fong JT, editor. *Fatigue Mechanisms.* ASTM STP 675. Philadelphia: ASTM; 1979. p. 69–105.

[18] Mughrabi H. Dislocations in fatigue. In: *Dislocations and properties of real materials*, Vol. 323. London: Institute of Metals; 1985, p. 244–262.

[19] Essmann U, Gösele U, Mughrabi H. A model of extrusions and intrusions in fatigued metals. Part I: Point defect production and the growth of extrusions. *Phil Mag A* 1981;**44**,405-426.

[20] Forsyth PJE. Slip-band damage and extrusion. *Proc R Soc Lond A*; 1957;**242**:198-202.

[21] Wood WA. Formation of fatigue cracks. *Phil Mag* 1958;**3**:692-699.

[22] Cottrell AH, Hull D. Extrusion and intrusion by cyclic slip in copper. *Proc R Soc Lond A* 1957;**242**:211-213.

[23] Laird C, Duquette DJ. Mechanisms of fatigue crack nucleation. In: Devereus OF, McEvily AJ, Staehle RW, editors. *Corrosion Fatigue,* NACE-2. Houston: National Association of Corrosion Engineers; 1972, p. 90-115.

[24] Mott NF. A theory of the origin of fatigue cracks. *Acta metall* 1958;**6**:195-197.

[25] Backofen WA. Formation of slip-band cracks in fatigue. In: Averbach BL, Felbeck, DK, G. T. Hahn GT, Thomas DA, editors. *Fracture.* Cambridge,Mass: MIT Press;1959, p. 435-447.

[26] Differt K, Essmann U, Mughrabi H. A model of extrusions and intrusions in fatigued metals. Part II: Surface roughening by random irreversible slip. *Phil Mag A* 1986;**54**, 237-258.

[27] Polák J. On the role of point defects in fatigue crack initiation. *Mater Sci Eng* 1987;**92**:71-80.

[28] Polák J. Cyclic deformation, crack initiation, and low-cycle fatigue. In: Ritchie RO, Murakami Y, editors. *Comprehensive Structural Integrity*, Oxford: Elsevier; 2003, p. 1-39.

[29] Basinski ZS, Basinski S. Fundamental aspects of low-amplitude cyclic deformation in face-centered cubic crystals. *Progr Mater Sci* 1992;**36**:89-148.

[30] Mughrabi H, Wang R, Differt K, Emann U. Fatigue crack initiation by cyclic slip irreversibilities in high-cycle fatigue . In: Lankford J, Davidson DL, Morris WL, Wei RP, editors. *Fatigue mechanisms: Advances in Quantitative Measurement of Fatigue Damage*. ASTM STP 811. Philadelphia: ASTM; 1983, p. 5-45.
[31] Brown LM. Dislocations and the fatigue strength of metals. In: Hartley CS, Ashby MF, Bullough R, Hirth JP, editors. *Proceedings of the International Conference on Dislocation Modeling of Physical Systems*, New York: Pergamon Press; 1980, p. 51–68.
[32] Hunsche A, Neumann P. Quantitative meurement of persistent slip band profiles and crack initiation. *Acta metall* 1986;**34**:207-217.
[33] Man J, Obrtlik K, Blochwitz C, Polák J. Atomic force microscopy of surface relief in individual grains of fatigued 316L austenitic stainless steel. *Acta mater* 2002;**50**:3767-3780.
[34] Polák J, AFM evidence of surface relief formation and models of fatigue crack nucleation. *Int J Fatigue* 2003;**25**:1027-1036.
[35] Man J, Obrtlik K, Polák J. Extrusions and intrusions in fatigued metals, Parts I & II. *Phil Mag* 2009;**89**:1295-1336 & 2009;**89**:1337-1372.
[36] Valiev R.Z., Islamgaliev R.K., Alexandrov I.V. Bulk nanostructured materials from severe plastic deformation. *Progr Mater Sci* 2000;45:103-189.
[37] Valiev RZ, Langdon TG. Principles of equal-channel angular pressing as a processing tool for grain refinement. *Progr Materials Sci* 2006;**51**:881-981.
[38] Mughrabi H, Höppel HW. Cyclic deformation and fatigue properties of ultrafine grain size materials: current status and some criteria for improvement of the fatigue resistance. *Mater Res Soc Symp Proc* 2001;**634**:B2.1.1- B2.1.12.
[39]Vinogradov AYu, Agnew SR In: *Nanocrystalline materials: fatigue. Dekker Encyclopedia of nanoscience and nanotechnology,* New York: Marcel Dekker, Inc.*;* 2004, p. 2269-2288.
[40] Höppel HW, Kautz M, Xu C, Murashkin M, Langdon TG, Valiev RZ, Mughrabi H. An overview: Fatigue behaviour of ultrafine-grained metals and alloys. *Int J Fatigue* 2005;**28**:1-10.
[41] Höppel HW, Mughrabi H, Vinogradov A. Fatigue properties of bulk nanostructured materials. In: Zehetbauer MJ, Zhu YT, editors. *Bulk nanostructured materials*. Weinheim: Wiley/VCH; 2009, p. 481-500.
[42] Mughrabi H, Höppel HW. Cyclic Deformation and Fatigue Properties of Very Fine-Grained Metal and Alloys. *Int J Fatigue*, doi:10.1016/j.ijfatigue.2009.10.007, in press.
[43] Dao M, Lu L, Asaro RJ, De Hosson JTM, Ma E. Toward a quantitative understanding of mechanical behavior of nanocrystalline metals. *Acta mater* 2007;**55**,4041–4065.
[44] Mughrabi H, Wang R. Cyclic stress-strain response and high-cycle fatigue behaviour of copper polycrystals, In: Lukáš P, Polák J, editors. *Proc. of International Colloquium on Basic Mechanisms in Fatigue of Metals*. Prague: Academia; 1988, p. 1-13.
[45] Thompson AW, Backofen AW. The Effect of Grain Size on Fatigue. *Acta metall* 1971;**19**:597-606.
[46] Staker MR, Holt DL. The dislocation cell size and dislocation density in copper deformed at temperatures between 25 and 700°C. *Acta metall.* 1972;**20**:569-579.
[47] Mughrabi H. On the grain-size dependence of metal fatigue: outlook on the fatigue of ultrafine-grained materials. In: Lowe TC, Valiev RZ, editors. *Investigations and applications of severe plastic deformation*, Dordrecht: Kluwer Academic Publishers; 2000, p. 241-253.
[48] Thiele E, Holste C, Klemm R. Influence of size effect on microstructural changes in cyclically deformed polycrystalline nickel. *Z Metallkd* 2002;**93**:730-736.
[49] Klemm R, Doctorate Thesis: *Zyklische Plastizität von mikro- und submikrokristallinem Nickel,* Technische Universität Dresden, 2004.
[50] Morrow JD. Cyclic plastic strain energy and fatigue of metals. In: *Internal Friction, Damping and Cyclic Plasticity*, ASTM STP 378; Philadelphia: ASTM; 1965, p. 45-87.
[51] Landgraf RW. The resistance of metals to cyclic deformation, In: *Achievement of High Fracture Resistance in Metals and Alloys*, ASTM STP 467; Philadelphia: ASTM; 1970, p. 3-36.
[52] Höppel HW. Mechanical properties of ultrafine grained metals under cyclic and monotonic loads: an overview. *Mater Sci Forum* 2006;**503-504**:259-266.
[53] Mughrabi H., Höppel H.W., Kautz M. Microstructural mechanisms governing the fatigue perfomance of ultrafine-grained metals and alloys. In: Zhu et al, editors. *Ultrafine Grained Materials IV.* Warrendale:TMS; 2006; p. 47-54.
[54] Agnew SR, Weertman JR. Cyclic softening of ultra fine grained copper. *Mater Sci Eng A* 1998;**244**:145-152.
[55] Vinogradov A, Kaneko Y, Kitagawa K, Hashimoto S, Stolyarov V, Valiev R. Cyclic response of ultrafine-grained copper at constant plastic strain amplitude. *Scripta Mater* 1997;**36**:1345-1351.
[56] Vinogradov A, Kaneko Y, Kitagawa K, Hashimoto S, Valiev RZ., On the cyclic response of ultrafine-grained copper. *Materials Science Forum* 1998; **269-272**: 987-992.
[57] Agnew SR, Vinogradov A, Hashimoto S, Weertman JR. Overview of fatigue performance of Cu processed by severe plastic deformation. *J Electron Mater* 1999;**28**:1038-1044.
[58] Höppel HW, Brunnbauer M, Mughrabi H, Valiev RZ, Zhilyaev AP. Cyclic deformation behaviour of ultrafine grain size copper produced by equal channel angular extrusion. In: *Proc. of Werkstoffwoche 2000*, *http://www.materialsweek.org/proceedings, 2001*.
[59] Höppel HW, Zhou ZM, Mughrabi H, Valiev RZ Microstructural study of the parameters governing coarsening and cyclic softening in fatigued ultrafine-grained copper. *Phil Mag A* 2002;**82**:1781-1794.
[60] Witney AB, Sanders PG, Weertman JR. Fatigue of nanocrystalline copper. *Scripta mater* 1995;**33**:2025-2030.
[61] Wang ZG, Wu SD, Jiang CB, Liu SM, Alexandrov IV. ECA pressing of copper single crystals and fatigue-induced softening in UFG metals. In: Blom AF, editor. *Proc. of FATIGUE 2002*, Vol. 3, West Midlands: Engineering Advisory Services; 2002, p. 1541-1552.
[62] Wu SD Wang ZG, Jiang CB, Li GY. Scanning electron microscopy-electron channelling contrast investigation of recrystallization during cyclic deformation of ultrafine grained copper produced by equal channel angular pressing. *Phil Mag Letters* 2002;**82**:559-565.
[63] Kunz L, Lukáš P, Svoboda M. Fatigue strength, microstructural stability and strain localization in ultrafine-grained copper. *Mater Sci Eng A* 2006;**424**:97-104.

[64] Lukáš P, Kunz L, Svoboda M, Buksa M, Wang Q. Mechanisms of cyclic plastic deformation in ultrafine-grain copper produced by severe plastic deformation. In: Hsia J, Göken M, Pollock T, Portella PD, Moody NR, editors. *Plasticity, Failure and Fatigue in Structural Materials – From Macro to Nano: Proceedings of the TMS Hael Mughrabi Honorary Symposium*. The Minerals, Metals and Materials Society (TMS); 2008, p. 161-166.
[65] Xu C, Wan Q, Zheng M, Li J, Huang M, Jia Q, Zhu J, Kunz L, Buksa M. Fatigue behaviour and damage characteristic of ultra-fine grain low-purity copper processed by equal channel angular pressing (ECAP). *Mater Sci Eng A* 2008; **475**:249-256.
[66] Shan A, Moon IG, Ko HS, Park JW. Direct observation of shear deformation during equal channel angular pressing of pure aluminium. *Scripta mater* 1999;**41**: 353-357.
[67] Lukáš P, Kunz L, Svoboda M. Fatigue of ultrafine-grained copper. In: Portella PD, Beck T, Okazaki M, editors. *Proc. of 6th Int Conf on Low Cycle Fatigue (LCF6)*. Berlin: DVM, Germany; 2008, p. 295-306.
[68] Höppel HW, Xu C, Kautz M, Barta-Schreiber N, Langdon TG, Mughrabi H. Cyclic deformation behaviour and possibilities to enhance the fatigue properties of ultrafine-grained materials. In: Zehetbauer MJ, Valiev RZ, editors. *Proceedings of 2nd International Conference on nanomaterials by severe plastic deformation (NanoSPD2),* Weinheim: Wiley VCH; 2004, p. 677-683.
[69] Kautz M, Höppel HW, Xu C, Langdon TG, Mughrabi H. Fatigue lives and cyclic deformation behaviour of ultrafine-grained materials. In: Portella P, Sehitoglu H and Hatanaka K, editors. *Proc 5th Int. Conf. on LCF Behaviour (LCF 5*), Berlin: DVM; 2004, p. 113-118.
[70] Wong MK, Kao WP, Lui JT, Chang CP, Kao PW. Cyclic deformation of ultrafine-grained aluminum. *Acta mater* 2007;**55**:715-725.
[71] Kunz L., Lukáš P. *Private communication*, 2009.
[72] Maier HJ, Gabor P, Gupta N, Karaman I, Haouaoui M. Cyclic stress-strain response of ultrafine grained copper. *Int J Fatigue* 2006;**28**:243-250.
[73] Lukáš P, Kunz L, Svoboda. Fatigue mechanisms in ultra-fine grained copper. *Konove mater* 2009;**47**:1-9.
[74] Mughrabi H, Höppel HW, Kautz M, Valiev RZ. Annealing treatments to enhance thermal and mechanical stability of ultrafine-grained metals produced by severe plastic deformation. *Z Metallkd* 2003;**94**:1079-1083.
[75] Wang, Y, Chen M, Zhou F, Ma E. High tensile ductility in a nanostructured metal. *Nature* 2002; **419**: 912-914.
[76] Höppel HW, Korn M, Lapovok R, Mughrabi H. Bimodal grain size distributions in UFG materials produced by SPD: Their evolution and effect on mechanical properties. In: *Proceedings of 15th Int Conf on Strength of Materials (ICSMA 15)*. To appear in: *Open Access Journal of Physics: Conference Series (JPCS).*
[77] Valiev RZ, Alexadrov IV, Zhu YT, Lowe TC. Paradox of strength and ductility in metals produced by severe plastic deformation. *J Mater Res* 2002;**17**:5-8.
[78] Lukáš P, Kunz L, Svoboda M, Fatigue notch sensitivity of ultrafine-grained copper. *Mater Sci Eng A* 2005;**391**:337-341.
[79] Hanlon T, Tabachnikova E.D, Suresh S. Fatigue crack growth behavior of nanocrystalline metals and alloys. *Int J Fatigue* 2005;**27**, 1147-1158.
[80] Hübner P, Kiessling R, Biermann H, Vinogradov A. Fracture behaviour of ultrafine-grained materials under static and cyclic loading. *Int J Mater Research* 2006;**97**:15661570.
[81] Hübner P, Kiessling R, Biermann H, Hinkel T, Jungnickel W, Kawalla R, Höppel HW, May J. Static and cyclic crack growth behaviour of ultrafine-grained Al produced by different severe plastic deformation methods. *Met Mater Trans A* 2007;**38**:1926-1933.
[82] Estrin Y, Vinogradov A. Fatigue behaviour of light alloys with ultrafine grain structure produced by severe plastic deformation: An overview. *Int J Fatigue* 2010; **32**, 898-907.
[83] Niendorf T, Canadinc D, Maier HJ, Karaman I. On the microstructural stability of ultrafine-grained interstitial-free steel under cyclic loading. *Met. Mater Trans. A* 2007;**38**:1946-1955.
[84] Mughrabi H. Cyclic deformation and fatigue of different steels: fundamentals and some examples of applications. In: Tsuji N, editor. *Proceedings of the 2nd Int Symp on Steel Science (ISSS 2009)*. In press.
[85] May J. Doctorate Thesis: *Mikrostruktur, monotone und zyklische mechanische Eigenschaften ultrafeinkörniger Aluminiumlegierungen*. Universität Erlangen-Nürnberg; 2008.
[86] Vinogradov AY, Stolyarov VV, Hashimoto S, Valiev RZ. Cyclic behavior of ultrafine-grain titanium produced by severe plastic deformation. *Mater Sci Eng A* 2001;**318**:163-173.
[87] Saitova LR, Höppel, HW, Göken M, Semenova IP, Valiev RZ. Cyclic deformation behavior and fatigue lives of ultrafine-grained Ti-6Al-4V ELI alloy for medical use. *Int J Fatigue* 2009;**31**:322-331.
[88] Furuya Y, Matsuoka S, Shimakura S, Hanamura T, Torizuka S. Effects of carbon and phosphorus addition on the fatigue properties of ultrafine-grained steels . *Scripta mater* 2005;**52**:1163-1167.
[89] Niendorf T, Canadinc D, Maier HJ, Karaman I, Sutter SG. On the fatigue behaviour of ultrafine-grained interstitial-free steel. *Int J Mat Res* 2006;**97**:1328-133.
[90] Selected papers from Proceedings of International Conference "Fatigue Life in Gigacycle Regime" (later called VHCF-1). *Fatigue & Fract Engng Mater Struct* 1999;**22**:545-641 and 1999;**22**:647-728.
[91] Mughrabi H. On the life-controlling microstructural fatigue mechanisms in ductile metals and alloys in the gigacycle regime. *Fatigue & Fract Engng Mater Struct* 1999;**22**:633-641.
[92] Mughrabi H. On multi-stage fatigue life diagrams and the relevant life-controlling mechanisms in ultrahigh-cycle fatigue. *Fatigue & Fract Engng Mater Struct* 2002;**25**:755-764.
[93] Mughrabi H. Specific features and mechanisms of fatigue in the ultrahigh-cycle regime. *Int J Fatigue* 2006;**28**:1501-1508.
[94] Stanzl-Tschegg S. Fracture mechanisms and fracture mechanics at ultrasonic frequencies. *Fatigue & Fract Engng Mater Struct* 1999;**22**:567-579.
[95] Murakami Y, Nomoto T, Ueda T, Murakami Y. On the mechanism of fatigue failure in the superlong life regime ($N>10^7$ cycles), Parts I and II. *Fatigue & Fract Engng Mater Struct* 2000;**23**:893-902 and 2000;**23**:903-910.

[96] Bathias C. There is no infinite fatigue life in metallic materials. *Fatigue & Fract Engng Mater Struct* 1999;**22**:559-565.
[97] Sakai T, Takeda M, Shiozawa K, Ochi Y, Nakajima M, Nakamura T and Ogyma N. Experimental evidence of duplex S-N characteristics in wide life region for high strength steels. In: Wu XR and Z.G. Wang ZG, editors. *Proc. of FATIGUE 1999*, Vol 1. Beijing: Higher Education Press and West Midlands: EMAS Ltd.;1999, p. 573-578.
[98] Nishijima S and Kanazawa K. Stepwise S-N curve and fish-eye failure in gigacycle fatigue. *Fatigue & Fract Engng Mater Struct* 1999;**22**:601-607.
[99] Lukáš P, Klesnil M, Polák J. High cycle fatigue life of metals. *Mater Sci Eng* 1974;**15**:239-245.
[100] Bathias C, Drouilac L, Le Francois P. How and why the fatigue S-N curve does not approach a horizontal asymptote. *Int J Fatigue* 2001;**23**:S143-S151.
[101] Furuya Y, Matsuoka S. Improvement of gigacycle fatigue properties by modified ausforming in 1600 and 2000 MPA-class low-alloy steels. *Metall Mater Trans A* 2002;**33**:3421-3431.
[102] Marines-Garcia, Paris PC, Tada H, BathiasC. Fatigue crack growth from small to long cracks in VHCF with surface initiations. *Int Fatigue* 2007;**29**:2072-2078.
[103] Mughrabi H, Wang, R. Cyclic deformation of face-centred cubic polycrystals: a comparison with observations on single crystals. In: Hansen N et al, editors. *Deformation of Polycrystals: Mechanisms and Microstructures, Proceedings of 2nd Risø International Symposium on Metallurgy and Materials Science*. Roskilde: Risø National Laboratory; 1981, p. 87-98.
[104] Höppel HW, Saitova L, Griess HJ, Göken M. In: Allison JE, Jones JW, Larsen JM, Ritchie RO. *Proc. 4th International Conference on Very High Cycle Fatigue (VHCF-4)*. Warrendale: TMS; 2007, p. 59-66, and *personal communication of H.W. Höppel*, 2008.
[105] Stanzl-Tschegg S, Mughrabi H, Schönbauer B. Life time and cyclic slip of copper in the VHCF regime. In: Bache et al editors. *Proceedings of International Conference on Fatigue Damage of Structural Materials*, 2006. *Int J Fatigue* 2007;**29**:2050-60.
[106] Mughrabi H, Stanzl-Tschegg S. Fatigue damage evolution in ductile single-phase face-centred cubic metals in the UHCF-Regime. In: Allison JE, Jones JW, Larsen JM, Ritchie RO. *Proc. 4th International Conference on Very High Cycle Fatigue (VHCF-4)*. Warrendale: TMS; 2007, p. 75-82.
[107] Weidner A, Amberger D, Pyczak F, Schönbauer B, Stanzl-Tschegg S, Mughrabi H. Fatigue damage in copper polycrystals subjected to ultrahigh-cycle fatigue below the PSB threshold. *Int J Fatigue* 2010;**32**:872-878.
[108] Stanzl-Tschegg S, Schönbauer B, Laird C. Mechanisms of fatigue failure of polycrystalline copper in the VHCF-regime. In: Hsia Jimmy K et al, editors. *Plasticity, Failure and Fatigue in Structural Materials – From Macro to Nano: Proceedings of the TMS Hael Mughrabi Honorary Symposium*. Warrendale: TMS; 2008, p. 229-34.
[109] Sonsino CM. Course of SN-curves especially in the high-cycle fatigue regime with regard to component design and safety. *Int J Fatigue* 2007;**29**:2246-2258.